# Combined Method for Rigid Bodies-Spring Model and Discrete Element Method

*** T.Yagi and N.Takeuchi [1], K.Yamamura[2], E.Hamasaki[3]**

[1] Graduate School of Engineering and Design, Hosei University, Tokyo, Japan.
[2] Nippon Steel & Sumitomo Metal Corporation, Chiba, Japan
[3] Advantechnology Co., Ltd., Miyagi, Japan

*Corresponding author: takeuchi@hosei.ac.jp

## Abstract

This paper presents a new method for a dynamic explicit scheme called as a combined RBSM-DEM. RBSM was developed as a numerical model for generalizing limit analysis in plasticity, in which a structure to be analyzed is idealized as an assemblage of rigid bodies connected by normal and tangential springs. Although the contact surfaces are handled differently by RBSM and DEM, the degree of freedom is the same. If the formulization using an explicit method for each element is used, the algorithms for dynamic analyses are identical. In this paper, we illustrate the formulization of RBSM that is expanded to include DEM. In addition, we examine the accuracy of the solutions obtained from some examples of numerical computations by the present method.

**Keywords:** RBSM, DEM, Combined model, Explicit method

## 1. Introduction

The implicit method is widely used for time integration in the numerical analysis of dynamic problems using the finite element method (FEM). On the other hand, the explicit method (Belytschko 1984), which involves the fracture problem, has also been extensively used. In this case, the time integration technique is represented by the central difference method, which calculates a solution sequentially. Recently, discontinuous analyses using the distinct element method (DEM) (Cundall 1971) and a combined DEM/FEM (Munjiza et al. 1995) have attracted considerable attention, and the use of the explicit scheme has increased. Therefore, a combined analysis technique is useful in the explicit method, and the same also applies to other numerical algorithms in a discontinuous problem.

The rigid bodies-spring model (RBSM) (Kawai 1977) was developed as a numerical model for generalizing the limit analysis in plasticity, in which a structure to be analyzed is idealized as an assemblage of rigid bodies connected by normal and tangential springs. Although contact surfaces are handled differently in RBSM and DEM, the degree of freedom is the same. If formulization by the explicit method for each element is used, the algorithms for dynamic analyses are identical.

This paper illustrates the formulization of RBSM for each element using the principle of hybrid virtual work. The same discussion is expanded to include DEM, and a method that combines RBSM and DEM is expressed. In addition, we numerically verify the stability and accuracy of the solutions obtained by a method that combines RBSM and DEM from some examples.

## 2. Discretization of equation of motion by using principle of hybrid virtual work

The basic equation of the elastic problem is as follows:

$$\operatorname{div} \boldsymbol{\sigma} + \boldsymbol{f} + \boldsymbol{f}_\alpha = 0 \ \text{ in } \ \Omega \tag{1}$$

$$\boldsymbol{\sigma} = \boldsymbol{D} : \boldsymbol{\varepsilon} \quad \boldsymbol{\varepsilon} = \boldsymbol{\nabla}^s \boldsymbol{u} \overset{\text{def.}}{=} \frac{1}{2}\left[\boldsymbol{\nabla}\boldsymbol{u} + (\boldsymbol{\nabla}\boldsymbol{u})^t\right]$$

$$\boldsymbol{u}|_{\Gamma_u} = \hat{\boldsymbol{u}} \ \text{(given)} \quad \boldsymbol{\sigma}|_{\Gamma_\sigma} \hat{\boldsymbol{n}} = \hat{\boldsymbol{t}} \ \text{(given)}$$

where $\Omega$ is the reference configuration of a continuum body with smooth boundary $\Gamma := \partial\Omega$; $\Gamma_u := \partial_u\Omega \subset \partial\Omega$, the geometrical boundary; $\Gamma_\sigma := \partial_\sigma\Omega \subset \partial\Omega$, the kinetic boundary; $\boldsymbol{\sigma}$, the Cauchy stress tensor; $\boldsymbol{\varepsilon}$, the infinitesimal strain tensor; $\boldsymbol{f}$, the body force per unit volume; $\boldsymbol{\nabla}$, the differential vector operator; and $\nabla^s$, the symmetric part of $\nabla$. When the displacement field in $\boldsymbol{x} \in \Omega$ is expressed as $\boldsymbol{u}$ and the density, as $\rho$, the inertia force $\boldsymbol{f}_\alpha$ of equation (1) is expressed as follows:

$$\boldsymbol{f}_\alpha = -\rho \frac{\partial^2 \boldsymbol{u}}{\partial t^2} \tag{2}$$

Let $\Omega$ consist of $M$ subdomains $\Omega^{(e)} \subset \Omega$ with the closed boundary $\Gamma^{(e)} := \partial\Omega^{(e)}$, as shown in Figure 1(a). In other words, $\Omega = \bigcup_{e=1}^{M} \Omega^{(e)}$; here, $\Omega^{(r)} \cap \Omega^{(q)} = 0 \quad (r \neq q)$ .

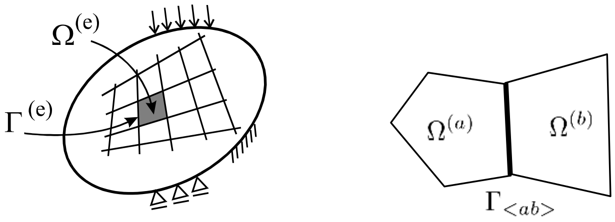


(a) subdomain $\Omega^{(e)}$ (b) common boundary $\Gamma_{<ab>}$

**Figure 1. Subdomain and its common boundary**

We use $\Gamma_{<ab>}$, defined as $\Gamma_{<ab>} \overset{\text{def.}}{=} \Gamma^{(a)} \cap \Gamma^{(b)}$, as the common boundary for two subdomains $\Omega^{(a)}$ and $\Omega^{(b)}$ adjoined as shown in Figure 1(b). The relation for the displacement $\tilde{\boldsymbol{u}}^{(e)}$ on $\Gamma_{<ab>}$, which is the intersection boundary between $\Omega^{(a)}$ and $\Omega^{(b)}$, is as follows:

$$\tilde{\boldsymbol{u}}^{(a)} = \tilde{\boldsymbol{u}}^{(b)} \ \text{ on } \ \Gamma_{<ab>} \tag{3}$$

The following hybrid-type virtual work equation is obtained by introducing this subsidiary condition into a virtual work equation using Lagrange multipliers $\boldsymbol{\lambda}$:

$$\begin{aligned} &\sum_{e=1}^{M} \left( \int_{\Omega^{(e)}} \boldsymbol{\sigma} : \mathrm{grad}(\delta \boldsymbol{u}) dV - \int_{\Omega^{(e)}} \boldsymbol{f} \cdot \delta \boldsymbol{u} \, dV - \int_{\Omega^{(e)}} \boldsymbol{f}_\alpha \cdot \delta \boldsymbol{u} \, dV \right) \\ &\quad - \sum_{s=1}^{N} \left( \delta \int_{\Gamma_{<s>}} \boldsymbol{\lambda} \cdot (\tilde{\boldsymbol{u}}^{(a)} - \tilde{\boldsymbol{u}}^{(b)}) \, dS \right) - \int_{\Gamma_\sigma} \hat{\boldsymbol{t}} \cdot \delta \boldsymbol{u} \, dS = 0 \qquad \forall \delta \boldsymbol{u} \in \mathbb{V} \end{aligned} \tag{4}$$

Here, $N$ denotes the number of common boundaries of the subdomain, and $\delta \boldsymbol{u}$ shows the virtual displacement. An independent displacement field in each subdomain is assumed as follows:

$$\begin{aligned} &\boldsymbol{u}^{(e)} = \boldsymbol{N}^{(e)} \boldsymbol{U}^{(e)} \\ &\boldsymbol{U}^{(e)} = \lfloor \boldsymbol{d}^{(e)}, \boldsymbol{\varepsilon}^{(e)} \rfloor^t \text{ , } \boldsymbol{N}^{(e)} = \lfloor \boldsymbol{N}_d^{(e)}, \boldsymbol{N}_\varepsilon^{(e)} \rfloor \end{aligned} \tag{5}$$

Here, $\boldsymbol{d}^{(e)}$ denotes the rigid displacement and the rigid rotation in point P in the subdomain ($e$), and $\boldsymbol{\varepsilon}^{(e)}$ denotes a constant strain in the subdomain ($e$). Equation (4) implies that the Lagrange multiplier $\boldsymbol{\lambda}$ is the surface force on the boundary $\Gamma_{<ab>}$ in subdomain $\Omega^{(a)}$ and $\Omega^{(b)}$; hence, the surface force is defined as follows:

$$\boldsymbol{\lambda}_{<ab>} = \boldsymbol{k} \cdot \boldsymbol{\delta}_{<ab>} \tag{6}$$

Here, $\boldsymbol{\delta}_{<ab>}$ shows the relative displacement on the boundary $\Gamma_{<ab>}$ , and $\boldsymbol{k}$ shows the penalty function. The equation of motion discretized about space by substituting the abovementioned relations in equation (4) is obtained as follows:

$$\begin{aligned} &\boldsymbol{M}\ddot{\boldsymbol{U}} + \boldsymbol{K}\boldsymbol{U} = \boldsymbol{P} \\ &\boldsymbol{M} = \sum_{e=1}^{M} \boldsymbol{M}^{(e)} \quad \boldsymbol{K} = \sum_{e=1}^{M} \boldsymbol{K}^{(e)} + \sum_{s=1}^{N} \boldsymbol{K}_{<s>} \end{aligned} \tag{7}$$

## 3. Method for combining RBSM and DEM

The formulization of RBSM is advanced by evaluating the energy stored in the spring between the adjoining elements as shown in Figure 2.

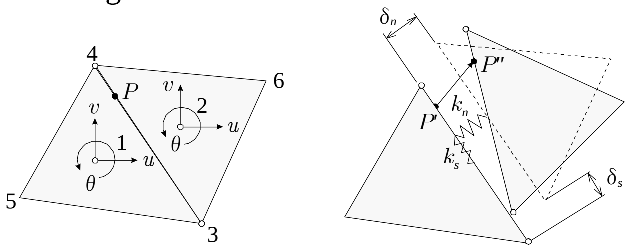


(a) before deformation (b) after deformation

**Figure 2. Rigid bodies-spring model**

The equation of motion (7) is simplified by $\boldsymbol{d}$ and $\boldsymbol{\varepsilon}$. Moreover, it is expressed in the global coordinate system as

$$\begin{bmatrix} \boldsymbol{M}_{dd} & \boldsymbol{M}_{d\varepsilon} \\ \boldsymbol{M}_{\varepsilon d} & \boldsymbol{K}_{\varepsilon\varepsilon} \end{bmatrix} \begin{Bmatrix} \ddot{\boldsymbol{d}} \\ \ddot{\boldsymbol{\varepsilon}} \end{Bmatrix} + \begin{bmatrix} \boldsymbol{K}_{dd} & \boldsymbol{K}_{d\varepsilon} \\ \boldsymbol{K}_{\varepsilon d} & \boldsymbol{K}_{\varepsilon\varepsilon} + \boldsymbol{D} \end{bmatrix} \begin{Bmatrix} \boldsymbol{d} \\ \boldsymbol{\varepsilon} \end{Bmatrix} = \begin{Bmatrix} \boldsymbol{P}_d \\ \boldsymbol{P}_\varepsilon \end{Bmatrix} \tag{8}$$

Here, the linear displacement field of equation (5), assuming a rigid displacement field and a mass matrix that contains only diagonal elements, is given as follows:

$$\boldsymbol{M}_{dd} = \rho \begin{bmatrix} A & 0 & 0 \\ 0 & A & 0 \\ 0 & 0 & I_p \end{bmatrix} \tag{9}$$

The substitution of the abovementioned relations into equation (8) gives

$$\boldsymbol{M}_{dd}\ddot{\boldsymbol{d}} = \boldsymbol{P}_d - \boldsymbol{K}_{dd}\boldsymbol{d} \tag{10}$$

In equation (6), $\boldsymbol{k}$ is the spring constant, and it is assumed as follows:

$$\begin{Bmatrix} \lambda_n \\ \lambda_s \end{Bmatrix} = \begin{bmatrix} k_n & 0 \\ 0 & k_s \end{bmatrix} \begin{Bmatrix} \delta_n \\ \delta_s \end{Bmatrix} \tag{11}$$

Here, under a plane stress condition, $k_n$ and $k_s$ are expressed as follows:

$$\left.\begin{aligned} \boldsymbol{k}_n &= \frac{E}{(1-\nu^2)(h1+h2)} \\ \boldsymbol{k}_s &= \frac{E}{(1+\nu)(h1+h2)} \end{aligned}\right\} \tag{12}$$

where $E$ is Young's modulus; $\nu$, Poisson's ratio; and *h*, the length of the vertical line to the boundary edge from the centroid of each subdomain.

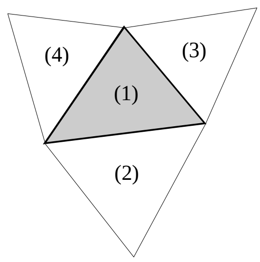


**Figure 3. Element (1) and adjoining element**

Here, as shown in Figure 3, we expand equation (11) as an example to element (1) and the adjoining element. In this case, the integration on the boundary edge, with a focus on element (1), is only relevant to elements (2)–(4). Therefore, the other elements are not relevant simultaneous equations. We represent a portion of equation (10) for this example as follows:

$$\begin{Bmatrix} \vdots \\ \boldsymbol{M}^{(1)} \\ \boldsymbol{M}^{(2)} \\ \boldsymbol{M}^{(3)} \\ \boldsymbol{M}^{(4)} \\ \vdots \end{Bmatrix} \begin{Bmatrix} \vdots \\ \ddot{\boldsymbol{d}}^{(1)} \\ \ddot{\boldsymbol{d}}^{(2)} \\ \ddot{\boldsymbol{d}}^{(3)} \\ \ddot{\boldsymbol{d}}^{(4)} \\ \vdots \end{Bmatrix} = \begin{Bmatrix} \vdots \\ \boldsymbol{P}_d^{(1)} \\ \boldsymbol{P}_d^{(2)} \\ \boldsymbol{P}_d^{(3)} \\ \boldsymbol{P}_d^{(4)} \\ \vdots \end{Bmatrix} - \begin{bmatrix} \ddots & & & & & \\ 0 & 3\boldsymbol{k}_{dd}^{(1,1)} & \boldsymbol{k}_{dd}^{(1,2)} & \boldsymbol{k}_{dd}^{(1,3)} & \boldsymbol{k}_{dd}^{(1,4)} & 0 \\ & \boldsymbol{k}_{dd}^{(1,2)} & \boldsymbol{k}_{dd}^{(2,2)} & & & \\ & \boldsymbol{k}_{dd}^{(1,3)} & & \boldsymbol{k}_{dd}^{(3,3)} & & \\ & \boldsymbol{k}_{dd}^{(1,4)} & & & \boldsymbol{k}_{dd}^{(4,4)} & \\ & & & & & \ddots \end{bmatrix} \begin{Bmatrix} \vdots \\ \boldsymbol{d}^{(1)} \\ \boldsymbol{d}^{(2)} \\ \boldsymbol{d}^{(3)} \\ \boldsymbol{d}^{(4)} \\ \vdots \end{Bmatrix} \tag{13}$$

Because $M^{(e)}$ is independent of each element, when focusing on element (1), the following relations are obtained.

$$\boldsymbol{M}^{(1)}\ddot{\boldsymbol{d}}^{(1)} = \boldsymbol{P}_d^{(1)} - \left(3\boldsymbol{k}_{dd}^{(1,1)}\boldsymbol{d}^{(1)} + \boldsymbol{k}_{dd}^{(1,2)}\boldsymbol{d}^{(2)} + \boldsymbol{k}_{dd}^{(1,3)}\boldsymbol{d}^{(3)} + \boldsymbol{k}_{dd}^{(1,4)}\boldsymbol{d}^{(4)}\right) \tag{14}$$

From the above relationship, the stress element is obtained using the surface forces of the element boundary, which can be expressed as follows:

$$\boldsymbol{M}^{(e)}\ddot{\boldsymbol{U}}^{(e)} = \boldsymbol{P}_d^{(e)} - \oint_{\Gamma^{(e)}} \boldsymbol{N}_d^{(e)}\boldsymbol{t}^{(e)}\, d\Gamma \tag{15}$$

Thus, the equation of motion becomes computable for each element. As shown in Figure 4, the element acceleration is obtained by the resultant of the contact forces in the case of discontinuous bodies.

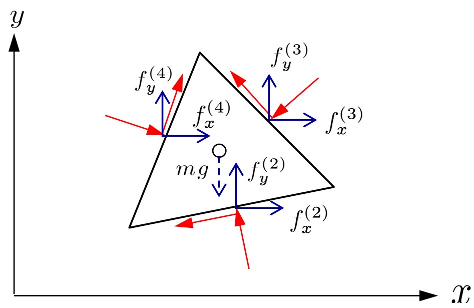


**Figure 4. Resultant of contact forces**

$$\ddot{\boldsymbol{u}}^{(e)} = \sum_{e=1}^{3} fx^{(e)}/m^{(e)} \tag{16}$$

$$\ddot{\boldsymbol{v}}^{(e)} = \sum_{e=1}^{3} fy^{(e)}/m^{(e)}$$

$$\ddot{\boldsymbol{\theta}}^{(e)} = \sum_{e=1}^{3} -(y-y_G)fx^{(e)} + (x-x_G)fy^{(e)}/I^{(e)}$$

The equation of motion (7) for the present time n is expressed as follows:

$$\boldsymbol{M}\ddot{\boldsymbol{U}}^{n} + \boldsymbol{K}\boldsymbol{U}^{n} = \boldsymbol{P}^{n} \tag{17}$$

Now, this formula is rewritten as follows:

$$\boldsymbol{M}\ddot{\boldsymbol{U}}^{n} = \tilde{\boldsymbol{P}}^{n} \tag{18}$$

This is a simplified form of equation (16) using the global coordinate system.
Here,

$$\widetilde{\boldsymbol{P}}^n = \boldsymbol{P}^n - \boldsymbol{F}^n \tag{19}$$

$$\boldsymbol{F}^n = \boldsymbol{K}\boldsymbol{U}^n \tag{20}$$

Equation (18) contains unknown acceleration parameters that can be obtained as follows:

$$\ddot{\boldsymbol{U}}^{n+1} = \boldsymbol{M}^{-1}\widetilde{\boldsymbol{P}}^n \tag{21}$$

Therefore, the following relations are obtained:

$$\dot{\boldsymbol{U}}^{n+1} = \dot{\boldsymbol{U}}^n + \ddot{\boldsymbol{U}}^{n+1}\Delta t \tag{22}$$

$$\boldsymbol{U}^{n+1} = \boldsymbol{U}^n + \dot{\boldsymbol{U}}^{n+1}\Delta t \tag{23}$$

The approach of equation (21), in a manner similar to DEM, is effective in solving collision problems. Thus, we can update the position of each element by looping $\Delta t$ in these calculations.

## 4. Numerical examples

As a numerical example, we present some simple problems.
First, we consider a laminated structure with a point load, as shown in Figure 5(a). In this example, we consider a brick block.
The material constants of this block are as follows: Young's modulus, 5127 N/mm$^2$; Poisson's ratio, 0.112; and density, 1850 kg/m$^3$. The incremental time is assumed to be $\Delta t = 5.0 \times 10^{-8}$ s. In addition, the load condition is constant.
The results for the displacement response on point A are shown in Figure 5(b). The blue solid line shows the results obtained by FEM, and the red dotted line shows those obtained by the present method. The results are almost identical.

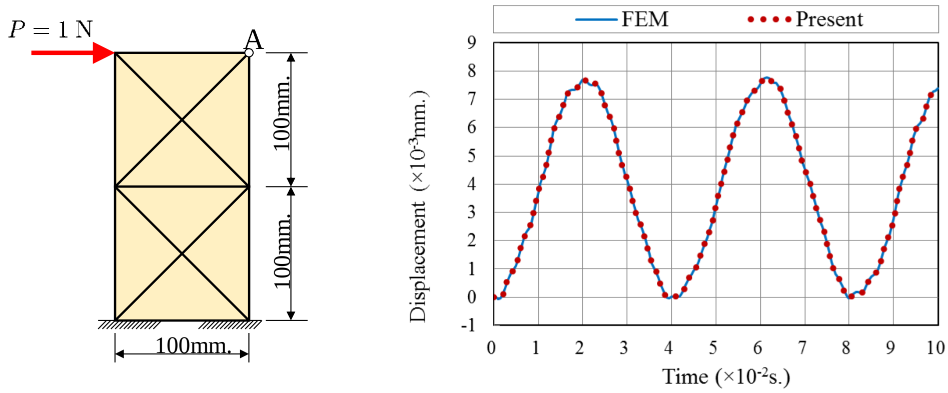


(a) model (b) deflection responses

**Figure 5. Case of elastic problem**

The next example is a problem involving hopping movement when a block is allowed to freely fall and collide with the ground, as shown in Figure 6(a). The gravitational acceleration is 9.80665 m/s$^2$. The material constants of this block are the same as those listed in the previous example. In this case, we assumed that no energy loss occurred from the block as a result of rebounding from the ground after the collision.
Figure 6(b) shows the status of contact point A when a brick block falls and hits the ground. The position was updated by repeated calculations when the length of ground penetration on the boundary side was larger than the allowable spring stiffness length, which verified the effect of the contact force. This result showed good agreement with the theoretical solution obtained by the equation of motion.

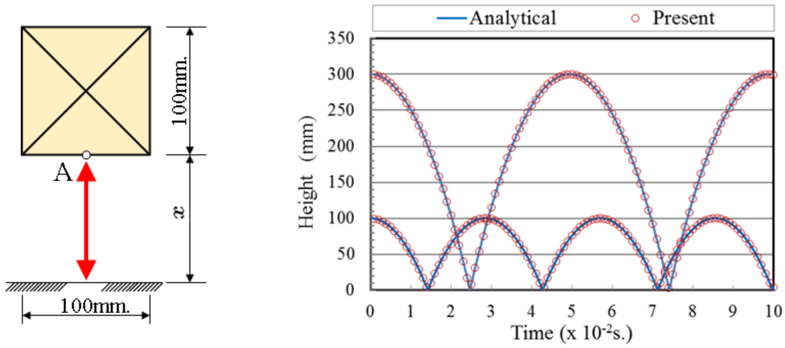


(a) model (b) update position

**Figure 6. Case of hopping movement**

The last example is a problem involving the sliding movement of a block on a slope in a gravitational field, as shown in Figure 7(a). We place a square block on slopes inclined at angles of θ = 5°, 15°, and 30° and let it slide down as shown in Figure 7(b). Again, the results of the present method are almost identical to those of the theoretical solution obtained by the equation of motion.

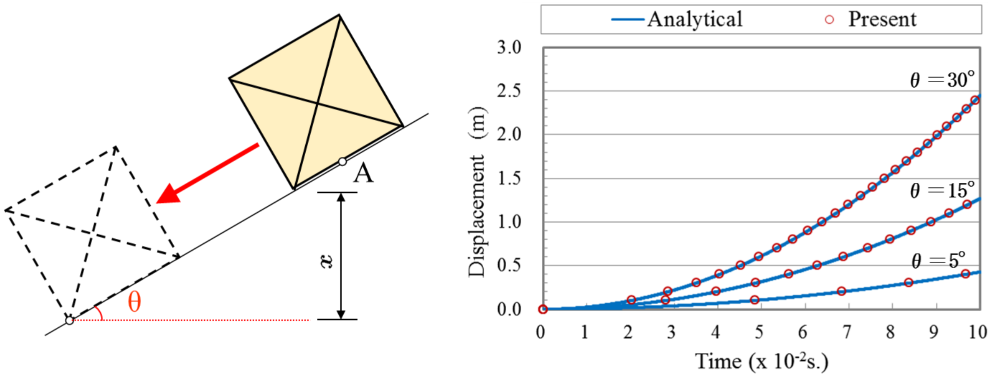


(a) model (b) update position

**Figure 7. Case of sliding movement**

## 5. Conclusions

This paper illustrated the formulization of RBSM for each element using the principle of hybrid virtual work. The same solution was also applied to DEM, and we developed a method that combined RBSM and DEM. As numerical examples, we first considered an elastic solution by using the present method, which had accuracy similar to that of FEM. Then, in a collision problem involving a falling block, we used the combined method for RBSM and DEM and expressed the effectiveness of the handling of the contact surface. Finally, from the behavior of a block sliding on a slope, we confirmed the applicability of the slip analysis.

### References

Belytschko, T., Lin, J.I. & Tsay, C.S. (1984), Explicit algorithms for the nonlinear dynamics of shells, *Computer Methods in Applied Mechanics and Engineering*, 42, pp.225–251.

Cundall, P.A. (1971), A computer model for simulating progressive, large scale movements in blocky rock systems, *Proceedings of the Symposium of International Society of Rock Mechanics*, 1(II-1), pp.129–136.

Munjiza, A., Owen, D.R.J. & Bicanic, N. (1995), A combined finite/discrete element method in transient dynamics of fracturing solids, *Engineering Computations*, 12, pp.145–174.

Kawai, T. (1977), New element models in discrete structural analysis, *Journal of the Society of Naval Architects of Japan*, 114, pp.1867–193.